

**$\mu$ SR study of magnetic order in the organic quasi-one-dimensional ferromagnet F4BImNN**Stephen J. Blundell,<sup>1,\*</sup> Johannes S. Möller,<sup>1</sup> Tom Lancaster,<sup>2</sup> Peter J. Baker,<sup>3</sup> Francis L. Pratt,<sup>3</sup> Gonca Seber,<sup>4</sup> and Paul M. Lahti<sup>4</sup><sup>1</sup>*Oxford University Department of Physics, Clarendon Laboratory, Parks Road, Oxford OX1 3PU, United Kingdom*<sup>2</sup>*University of Durham, Centre for Materials Physics, South Road, Durham, DH1 3LE, United Kingdom*<sup>3</sup>*ISIS Facility, STFC Rutherford Appleton Laboratory, Chilton, Oxfordshire OX11 0QX, United Kingdom*<sup>4</sup>*Department of Chemistry, University of Massachusetts, Amherst, Massachusetts 01003, USA*

(Received 15 May 2013; revised manuscript received 7 August 2013; published 27 August 2013)

The stable organic radical 2-(4,5,6,7-tetrafluorobenzimidazol-2-yl)-4,4,5,5-tetramethyl-4,5-dihydro-1*H*-imidazole-3-oxide-1-oxyl (F4BImNN) forms hydrogen-bonded chains in the solid state and exhibits one-dimensional ferromagnetic exchange with  $J/k_B = 22$  K. We use muon-spin rotation to demonstrate that weak interchain interactions drive the system to long-range magnetic order below  $T_c = 0.72$  K. We use density-functional calculations of the muon site and compare our results to those obtained on the nonfluorinated analog compound. Our results show that F4BImNN is the best realization of a one-dimensional Heisenberg ferromagnet among purely organic compounds yet discovered.

DOI: 10.1103/PhysRevB.88.064423

PACS number(s): 75.50.Xx, 76.75.+i, 75.10.Pq

**I. INTRODUCTION**

Purely organic or molecular magnets<sup>1–4</sup> show a range of extremely rich behavior, and any specific property, once identified in a particular system, can then be tuned using pressure<sup>5</sup> or by chemical techniques.<sup>6–8</sup> One aspect of this research field is the quest for purely organic ferromagnets, which has succeeded at least in producing some excellent model systems of varying dimensionalities, though transition temperatures are low.<sup>9–12</sup> One family of interesting magnets can be constructed using nitronyl nitroxide radicals<sup>9,13</sup> since a variety of organic groups can be attached to the nitronyl nitroxide neutral radical in order to produce different crystal architectures which can favor or inhibit particular intermolecular interactions.

An attractive route to synthesize quasi-one-dimensional (quasi-1D) magnets involves benzimidazoles which readily form chains due to  $\text{NH} \cdots \text{H}$  interactions between the NH donor on one molecule and the azole N acceptor on its neighbor [Fig. 1(c)]. The molecule BImNN<sup>14</sup> [molecular structure shown in Fig. 1(a)] exhibits ferromagnetic interactions in the solid state.<sup>15–17</sup> The ferromagnetic interactions result from the overlap between spin density on oxygen on the nitronyl nitroxide group of one molecule and the central carbon of the nitronyl nitroxide group of its neighbor [Fig. 1(d)].<sup>15,18</sup> A related compound, which only differs from BImNN by one benzene ring, shows antiferromagnetic and not ferromagnetic interactions,<sup>17</sup> thus demonstrating the important role of crystal packing. One method to tune BImNN is to substitute F for H on the benzenoid ring, thereby changing the polarity of the substituent groups, but leaving the crystal packing relatively (but not completely) unchanged. The resulting molecule, F4BImNN [Fig. 1(b)] which we study here, thus also exhibits quasi-one-dimensional chain formation and similar ferromagnetic exchange to BImNN.<sup>19</sup> BImNN and F4BImNN can be chemically alloyed<sup>20</sup> producing  $(\text{F4BImNN})_x(\text{BImNN})_{1-x}$ . BImNN-rich alloys ( $x < 0.8$ ) have an orthorhombic unit cell (space group  $Pbca$ ) while the F4BImNN-rich compositions ( $x > 0.9$ ) yield<sup>21</sup> monoclinic unit cells ( $P2_1/c$ ). Nevertheless, the intermolecular packing remains dominated by the hydrogen-bonded chains and leads to quasi-1D ferromagnetic

exchange. Application of hydrostatic pressure to F4BImNN results in an increase of the intrachain exchange  $J$  (by about 50% in 10 kbar).<sup>22</sup>

In a one-dimensional Heisenberg magnet one may write the Hamiltonian  $\mathcal{H}$ ,

$$\mathcal{H} = -J \sum_{\langle i,j \rangle} \mathbf{S}_i \cdot \mathbf{S}_j - J' \sum_{\langle i,i' \rangle} \mathbf{S}_i \cdot \mathbf{S}_{i'}, \quad (1)$$

where the first sum double counts intrachain interactions, controlled by the intrachain exchange constant  $J$ , and the second sum double counts interactions between the chains, controlled by the interchain exchange constant  $J'$ . (Note that this paper uses the “ $2J$ ” convention in which two exchange-coupled spin- $\frac{1}{2}$  moments have an energy splitting of  $2J$  between singlet and triplet levels.) It is notable that  $J/k_B \approx 22$  K in both BImNN and F4BImNN<sup>17,20</sup> so that differences in magnetic ordering between the two contributions can be attributed to differences in packing which influence the interchain interactions  $J'$ ; thus the substitution of H by F can play an important role. In this paper we report muon-spin rotation ( $\mu$ SR) experiments (Sec. II) on F4BImNN that demonstrate long-range magnetic order at low temperature (Sec. III). By using density-functional theory calculations of the muon site (Sec. IV), we compare experimental results for BImNN and F4BImNN (Sec. V).

**II. EXPERIMENTS**

$\mu$ SR experiments<sup>23</sup> are effective at establishing three-dimensional ordering in low-dimensional magnets because below the transition a spontaneous precession of the muon spin-polarization can be observed in zero field; see, e.g., Refs. 24–27. Thermodynamic measurements are frequently dominated by the effect of intrachain interactions (for example, three-dimensional ordering in a very anisotropic spin chain is associated with a tiny fraction of the total entropy since, on cooling, very long correlated segments develop on individual chains in advance of the condensation of long-range order<sup>28</sup>). Our  $\mu$ SR experiments were carried out using the HiFi (high field) spectrometer at the ISIS Pulsed Muon Facility at the

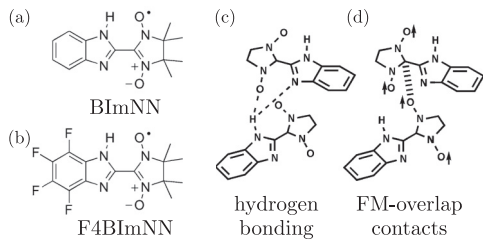


FIG. 1. The molecular structure of (a) BImNN and (b) F4BImNN. (c) The hydrogen bonding interactions that link the molecular chains and (d) the ferromagnetic overlaps, after Ref. 22.

Rutherford Appleton Laboratory which is equipped with a dilution refrigerator. In our  $\mu$ SR experiment, spin polarized positive muons ( $\mu^+$ , momentum 28 MeV/c) were implanted into an array of randomly oriented very small crystals of F4BImNN. The muons stop quickly (in  $<10^{-9}$  s), without significant loss of spin polarization. The observed quantity is then the time evolution of the average muon spin polarization  $P_z(t)$ , which can be inferred<sup>23</sup> via the asymmetry in the angular distribution of emitted decay positrons, parameterized by an asymmetry function  $A(t)$  proportional to  $P_z(t)$ .

### III. RESULTS

Example  $\mu$ SR spectra from F4BImNN are presented in Fig. 2(a) and show that a clear precession signal is observed at low temperature, signifying the presence of long-range magnetic order due to a quasistatic magnetic field being present at least at one muon site. The data are superficially similar to those obtained for BImNN.<sup>29</sup> The data are well described by

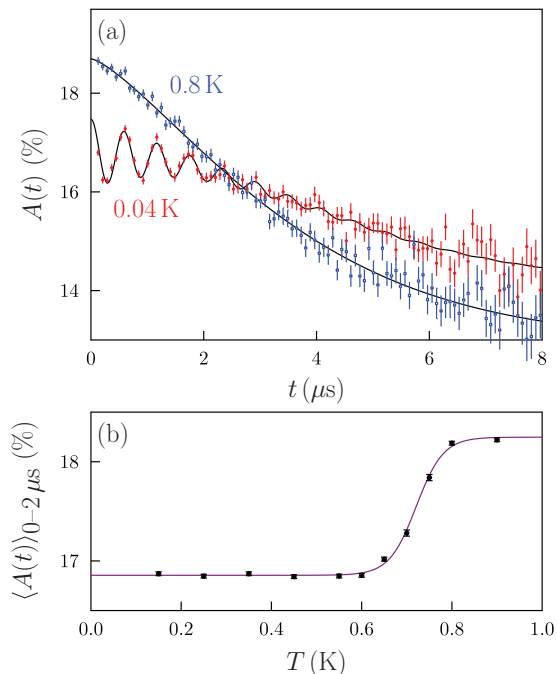


FIG. 2. (Color online) (a) Example  $\mu$ SR spectra [the asymmetry function] for F4BImNN measured above and below the magnetic transition. (b) Because the oscillations disappear before the transition is reached, the transition can be identified by plotting the average value of  $A(t)$  over the first two microseconds of data.

the fitting function

$$A(t) = A_1 e^{-\Delta t} \cos(2\pi \nu t) + A_2 e^{-\sigma^2 t^2} + A_{bg}, \quad (2)$$

where  $\nu$  is the muon precession frequency (equal to  $\gamma_\mu B/2\pi$ , with  $B$  the magnetic field at the muon site and  $\gamma_\mu = 2\pi \times 135.5 \text{ MHz T}^{-1}$ ) and  $A_{bg}$  the background contribution from those muons that stop outside the sample. The first term, with amplitude  $A_1$ , arises from those muons that stop in positions of quasistatic magnetic order with their spin components perpendicular to the local magnetic field at the muon site (expected to be 2/3 of the total in a polycrystalline sample). The amplitude  $A_1$  is zero above  $T_c$  and nonzero below  $T_c$ . A nonoscillatory component of amplitude  $A_1/2$  is also expected, originating from the same muon sites but representing the cases in which the muon spin is oriented parallel to the local field (and this would normally be expected to show exponential relaxation due to spin-lattice relaxation). The data show that  $A_2$  is considerably larger than  $A_1/2$  and so the nonoscillatory contribution with amplitude  $A_2$  must additionally contain signal from some other site(s) giving rise to predominantly Gaussian relaxation. (In our fits, in the temperature range up to  $\sim 0.55$  K in which Eq. (2) described the data, the total relaxing asymmetry,  $A_1 + A_2$ , was in the range 3.5%–4%, with  $A_1$  always about 0.6%). The measured initial asymmetry is also reduced from the expected maximum for the HiFi spectrometer ( $\approx 22\%$ ) and so there is probably another site in which the muon is strongly coupled to a large local field, possibly forming a paramagnetic state which is known to occur in some nitronyl nitroxide systems.<sup>30</sup> Thus the form of the relaxation probably reflects a variety of realized muon stopping sites, only one of which gives rise to measurable oscillations. We note that a very similar form for the relaxation was obtained in  $\mu$ SR experiments on BImNN.<sup>29</sup> Although F4BImNN contains fluorine atoms, we do not see any evidence for F- $\mu$ -F states in the zero-field data which have been identified in data on many ionic fluorides,<sup>31</sup> molecular magnets,<sup>27</sup> and in the polymer PTFE,<sup>32</sup> as well as in density-functional calculations of muon stopping sites in fluorides.<sup>33,34</sup> Because the fluorines are covalently bonded to a conjugated ring, they become less attractive stopping sites for muons than would be the case in, for example, an ionic fluoride.

Fits to Eq. (2) for data sets at different temperatures yield the evolution of the precession frequency in F4BImNN, and this is plotted in Fig. 3 together with analogous data for BImNN (from Ref. 29). The damping of the oscillating component increases on warming and oscillations become unresolvable above about 0.55 K. Thus, as found for BImNN,<sup>29</sup> it is not possible to extract a precession signal close to the magnetic transition. However, the shape of the spectra change more dramatically as the sample is warmed through 0.7 K and so the data are consistent with a magnetic transition at 0.7 K, in agreement with ac susceptibility and heat capacity data<sup>18</sup> which identify a phase transition at 0.72 K. An estimate of the transition temperature from our data can be obtained by studying the average of the initial part (chosen here to be the first 2  $\mu$ s) of the  $\mu$ SR spectra which are the most sensitive to the fast relaxation due to magnetic order. This is plotted in Fig. 2(b) and shows a crossover with a fitted midpoint of 0.721(4) K and a width of 0.06 K, in excellent agreement

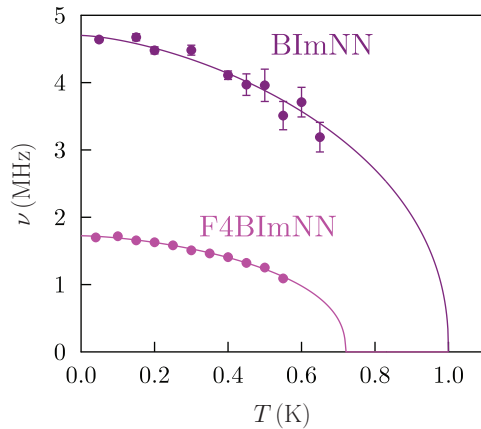


FIG. 3. (Color online) Temperature evolution of the precession frequency of the  $\mu$ SR spectra in F4BImNN for  $T < T_c$  from fits to Eq. (2). Also shown are the analogous data for BImNN (from Ref. 29).

with the previous studies.<sup>18</sup> The fitted lines in Fig. 3 use the phenomenological form  $\nu(T) = \nu(0)[1 - (T/T_c)^\alpha]^\beta$  with  $T_c$  set to the values identified by Refs. 18 and 29 and yield  $\alpha \approx 1.5$  and  $\beta = 0.3-0.4$  for both compounds, values which are consistent with three-dimensional ordering (although the lack of data close to the transition precludes further analysis or interpretation). The volume per spin for F4BImNN is about 10% larger than in BImNN, reflecting the increased chemical pressure,<sup>21</sup> but the reduced  $T_c$  is due to a subtle tuning between intermolecular contacts. We note also that, for both BImNN and F4BImNN, the critical temperature  $T_c$  representing three-dimensional ordering is probably a Néel temperature  $T_N$  so that the ferromagnetic chains couple antiferromagnetically, as suggested by ac susceptibility measurements.<sup>18,21</sup>

#### IV. MUON SITE CALCULATIONS

We have performed density-functional theory (DFT) calculations to investigate the location of the muon in F4BImNN and BImNN. The calculations were performed with the QUANTUM ESPRESSO package<sup>35</sup> within the generalized-gradient approximation<sup>36</sup> (GGA) using norm-conserving and ultrasoft<sup>37</sup> pseudopotentials. The muon was modeled by a norm-conserving hydrogen pseudopotential. The wave function and charge-density cutoffs were 80 and 320 Ry, respectively. Brillouin-zone integration was performed at the  $\Gamma$  point. The results reported were obtained from calculations for the conventional unit cell (plus the muon). The system was assumed to be neutral for the calculation, but calculations performed on a charged (+1) unit cell (compensated by a uniform background charge) revealed similar results. The muon was placed in many randomly chosen sites and all atoms were allowed to relax. The structural relaxations were based on the structures measured at 100 K, reported previously.<sup>21</sup> For the unit cell without the muon we have found small relaxations of the hydrogen and fluorine atoms by approximately 0.12 and 0.05 Å, respectively [leading to an energy gain of approximately 0.1 (F4BImNN), 0.15 (BImNN) eV/atom in the process]. No significant enthalpy gain (<10 meV/atom) was observed when the unit cell was allowed to relax without the

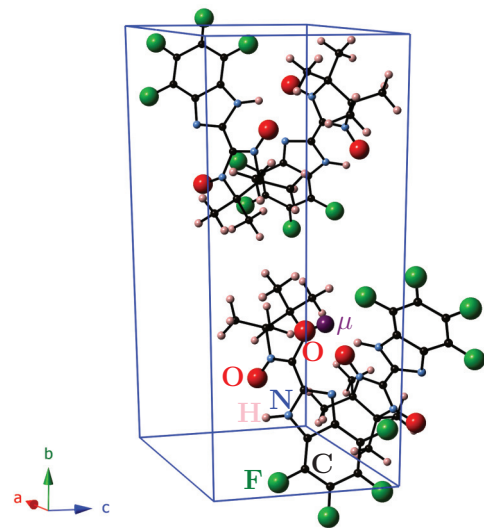


FIG. 4. (Color online) The “ $O_A$  site” of the muon in F4BImNN. Molecules from within the unit cell are shown completely (including their fragments in neighboring cells). Molecular fragments from neighboring unit cells are hidden. The oxygen the muon bonds to is distorted by 1.3 Å from its position in the unperturbed bulk; the neighboring fluorines are distorted by up to 0.8 Å. For the “ $O_B$  site,” the muon bonds to the other labeled oxygen on the nitronyl group.

muon, and therefore the experimental unit cell parameters were used. Structural relaxations were performed in a non-spin-polarized calculation, but no significant additional relaxation was found in a spin-polarized calculation; all structures and energies discussed below are for the non-spin-polarized calculation.

The structural relaxations predict three low-energy sites for the muon in both F4BImNN and BImNN: (i) the “ $O_A$  site” where the muon forms a covalent bond with the oxygen in the nitronyl nitroxide group (see Fig. 4), (ii) the “nitrogen site” where the muon forms a covalent bond with the vacant nitrogen and hydrogen-bonds to the  $O_A$  in the nitronyl nitroxide group, and (iii) the “ $O_B$  site” where the muon bonds to the other oxygen in the nitronyl nitroxide group. We note that, in agreement with the experimental data, the formation of an F- $\mu$ -F state is not predicted. In F4BImNN the lowest energy site is the nitrogen site, with the  $O_A$  and the  $O_B$  sites being approximately 70 and 170 meV higher in energy; in BImNN the  $O_A$  and the nitrogen site are degenerate within the accuracy of the calculation and the  $O_B$  site is approximately 40–80 meV higher in energy. These energies do not take account of the large zero-point energy (ZPE) of the muon, recently shown to be as large as 0.8 eV in the F- $\mu$ -F molecule.<sup>33</sup> Unfortunately a full calculation of the vibrational modes of the crystal in analogy to Ref. 33 is prohibitive due to the size of the unit cell. We have made a rough estimate of the ZPE (in the harmonic approximation) for the three sites found above by calculating the vibrational modes of the molecule in vacuum, with and without muon and taking the difference of the total ZPE. The additional ZPE of the molecule with the muon is between 0.9 and 1.0 eV for all three sites. Since this calculation neglects the intermolecular coupling, these estimates allow no further distinction between the three candidate sites. Given the size

of the ZPEs for all of the three candidate sites and the small differences in “classical” energies above, we conclude that, within the accuracy of our calculation, the three candidate sites are approximately degenerate. We note that this is in agreement with the experimental observation that a number of muon sites are realized, only one of which gives rise to oscillations in the muon decay asymmetry.

## V. DISCUSSION

A clear result of Fig. 3 is that the frequency of the precession signal extrapolated to zero temperature is substantially lower in F4BImNN as compared with BImNN. This supports the notion that the muon site giving rise to the observed precession in both compounds lies between the chains. All of our candidate muon sites lie somewhat between chains, albeit bonded to one particular molecule. Although the crystallographic packing of molecules within chains is very similar for BImNN and F4BImNN, there is a substantial difference between the two in the way chains are stacked together.<sup>18</sup> This arises because CF units in F4BImNN form favorable contacts with the methyl groups adjacent to the nitronyl nitroxide groups, whereas in BImNN the dominant interchain contacts are methyl-methyl and aryl-aryl.<sup>18,21</sup> The net result is that the chains are offset in different ways, displaced with respect to each other along the ferromagnetic stacking axis, and thus it is plausible that this effect gives rise to different contributions from the ordered spins to the dipolar field measured at the muon site, although it is also possible that the slightly greater degree of one-dimensionality in F4BImNN could result in a more reduced moment owing to increased fluctuations.

To understand this in more detail we have estimated the dipolar field at all three sites for both F4BImNN and BImNN for several trial magnetic structures consistent with ferromagnetic order within each chain: (i) antiferromagnetic interactions between the chains, resulting in Néel order within the plane; (ii) all chains ferromagnetically aligned, resulting in a bulk ferromagnet; (iii) chains ferromagnetically aligned along one interchain direction but antiferromagnetically aligned along the other. The first structure is most likely as it minimizes the total dipolar energy and is consistent with the bulk data, but calculations were performed for all three structures. We have used Hartree Fock (UHF/PM3) and Gaussian DFT (B3LYP/cc-pVDZ) calculations of the isolated molecule of F4BImNN and found that muonium addition at O<sub>A</sub> and O<sub>B</sub> gives rise to a local electronic singlet and so only dipolar coupling is expected. A nonzero contact hyperfine coupling is predicted for the nitrogen site and this could account for the observed missing asymmetry. However, this nonzero contact hyperfine coupling could not be reproduced in our GGA solid state calculations which predict all three sites to have negligible contact hyperfine coupling.

The dipolar field was calculated by assuming localized moments on each of the atoms of the nitronyl nitroxide group with the magnitude (and sign) of the moment obtained from a Löwdin population analysis and ignoring any renormalization of the moment due to quantum fluctuations. For both F4BImNN and BImNN the Löwdin analysis yielded spin-only moments of approximately 0.31, 0.25,  $-0.1$ , 0.26, and 0.27  $\mu_B$

on oxygen, nitrogen, central carbon, nitrogen, and oxygen (reading across the nitronyl nitroxide group), respectively, in fair agreement with the Mulliken analysis presented for the F4BImNN molecule previously.<sup>21</sup> The muon significantly distorts the crystal structure locally in all three sites, even though it forms a covalent bond, which partially screens the muon charge. For the O<sub>A</sub> and O<sub>B</sub> sites the presence of the muon destroys the spin polarization on the host molecule since the unpaired electron is removed from the radical but leaves the spin density on the surrounding molecules almost unperturbed. For the muon in the nitrogen site, our calculations suggested a less localized perturbation of the magnetic structure. In all dipolar-field calculations the muon-induced structural and magnetic relaxations were included within one unit cell and all surrounding unit cells were assumed unrelaxed, an excellent approximation as muon-induced effects are extremely short ranged. For BImNN we have found reasonable agreement with the experimental oscillation frequency for all of the sites for most of the trial magnetic geometries, for example for Néel order with ferromagnetic alignment along the chain, the dipolar coupling for a muon in the O<sub>A</sub> site would be approximately 3.4, 5.2, or 4.4 MHz for moments along  $a$ ,  $b$ ,  $c$ , respectively. For F4BImNN only the O<sub>A</sub> site (Fig. 4) affords dipolar couplings that are consistent with the experimental value of approximately 1.75 MHz. For Néel order this coupling would be approximately 3.4, 3.0, 1.0 MHz for magnetic moments along  $a^*$ ,  $b$ ,  $c$ . In fact, the dipolar anisotropy gives an energetic preference for the moments to be parallel to the chain direction ( $a$  for BImNN and  $c$  for F4BImNN). Thus our calculations would predict  $\nu(0) = 3.4$  MHz for BImNN and  $\nu(0) = 1.0$  MHz for F4BImNN. The experimental values are slightly higher (4.7 and 1.75 MHz respectively) but the calculations successfully reproduce the smaller  $\nu_\mu$  for F4BImNN. The discrepancy between observed and calculated dipolar coupling is likely due to small errors in precisely determining the geometry of the muon site and the magnetic moments, though using the spin-only moments obtained in a previous Mulliken analysis<sup>21</sup> gives qualitatively similar

TABLE I. Magnetic properties of selected one-dimensional ferromagnets.  $\gamma$  phase  $p$ -NPNN = para-nitrophenyl nitronyl nitroxide, Me = CH<sub>3</sub>, DMSO = C<sub>2</sub>H<sub>6</sub>SO,  $p$ -CDTV = 3-(4-chlorophenyl)-1,5-dimethyl-6-thioverdazyl, TMSO = C<sub>4</sub>H<sub>8</sub>SO, CHAC = C<sub>6</sub>H<sub>11</sub>NH<sub>3</sub>CuCl<sub>3</sub>,  $p$ -CDpOV = 3-(4-chlorophenyl)-1,5-diphenyl-6-oxoverdazyl, TMCuC = tetramethylammonium copper trichloride, and CHAB = C<sub>6</sub>H<sub>11</sub>NH<sub>3</sub>CuBr<sub>3</sub>.

Compound	Reference	$J/k_B$ (K)	$T_c$ (K)	$k_B T_c/J$
$\gamma$ phase $p$ -NPNN	38	2.15	0.65	0.30
Me <sub>3</sub> NHCuCl <sub>3</sub> ·2H <sub>2</sub> O	39	0.85	0.165	0.19
CuCl <sub>2</sub> (DMSO)	40,41	45	4.8	0.11
$p$ -CDTV	42	6.0	0.67	0.11
CuCl <sub>2</sub> (TMSO)	40,41	39	3	0.08
CHAC	43,44	45–53	2.18	0.04–0.05
$p$ -CDpOV	45	5.5	0.21	0.038
TMCuC	41,46,47	30, 45	1.24	0.03–0.04
CHAB	48	55	1.50	0.027
BImNN	29	22	1.0	0.045
F4BImNN	This work	22	0.72	0.033

results. It is important to note that ignoring the muon-induced structural and magnetic relaxation completely would have led to predictions of  $\nu(0) = 21.9$  MHz for BImNN and  $\nu(0) = 22.6$  MHz for F4BImNN, greatly in excess of the experimental values. This demonstrates that the muon-induced effects have to be included.

We have found that the field at the muon site reflects a balance between competing terms: (i) the field due to the molecule to which the muon is bonded (sometimes very low if the muon destroys the spin polarization on the host molecule) and is usually antiparallel to the moment on the molecule; (ii) the field due to the neighboring molecules within the same chain, usually parallel to the moments that lie along the chain; (iii) the field due to molecules in different chains, which can be parallel or antiparallel to the moments along the chain containing the muon, depending on the magnetic structure and the way the chains are packed together. It is this delicate balance that means that the difference in the crystallographic packing of chains between BImNN and F4BImNN give rise to the different  $\nu(0)$  observed in experiment and reproduced in the DFT calculations.

The results obtained in this paper also allow us to compare the values of intrachain exchange constant  $J$ , three-dimensional ordering transition temperature  $T_c$ , and the ratio  $k_B T_c / J$  for various quasi-one-dimensional ferromagnets in Table I. This latter quantity is a measure of the one-dimensional nature of the ferromagnetism. It is readily seen that F4BImNN, with a value of  $J$  large for a purely organic system but its low  $T_c$ , has a remarkably low value of  $k_B T_c / J$ , and lower than BImNN. It is therefore among the most strongly one-dimensional of the spin- $\frac{1}{2}$  ferromagnetic chains so far synthesized and we believe it now holds the record among purely organic magnets.

## ACKNOWLEDGMENTS

We thank Davide Ceresoli and Nicola Marzari for useful discussions. We thank the E-Infrastructure South Initiative for CPU time and STFC (ISIS) for beam time. This work is supported by the EPSRC, UK and the National Science Foundation under Grant No. CHE 0809791.

---

\*Corresponding author: s.blundell@physics.ox.ac.uk

<sup>1</sup>*Magnetic Properties of Organic Materials*, edited by P. M. Lahti (Dekker, New York, 1999).

<sup>2</sup>S. J. Blundell and F. L. Pratt, *J. Phys.: Condens. Matter* **16**, R771 (2004).

<sup>3</sup>M. Kurmoo, *Chem. Soc. Rev.* **38**, 1353 (2009).

<sup>4</sup>J. S. Miller, *Chem. Soc. Rev.* **40**, 3266 (2011).

<sup>5</sup>M. Mito, H. Deguchi, T. Tanimoto, T. Kawae, S. Nakatsuji, H. Morimoto, H. Anzai, H. Nakao, Y. Murakami, and K. Takeda, *Phys. Rev. B* **67**, 024427 (2003).

<sup>6</sup>M. Deumal, J. Cirujeda, J. Veciana, and J. J. Novoa, *Chem. Eur. J.* **5**, 1631 (1999).

<sup>7</sup>P. A. Goddard, J. L. Manson, J. Singleton, I. Franke, T. Lancaster, A. J. Steele, S. J. Blundell, C. Baines, F. L. Pratt, R. D. McDonald, O. E. Ayala-Valenzuela, J. F. Corbey, H. I. Southerland, P. Sengupta, and J. A. Schlueter, *Phys. Rev. Lett.* **108**, 077208 (2012).

<sup>8</sup>C. J. Wedge, G. A. Timco, E. T. Spielberg, R. E. George, F. Tuna, S. Rigby, E. J. L. McInnes, R. E. P. Winpenny, S. J. Blundell, and A. Ardavan, *Phys. Rev. Lett.* **108**, 107204 (2012).

<sup>9</sup>M. Tamura, Y. Nakazawa, D. Shiomi, K. Nozawa, Y. Hosokoshi, M. Ishikawa, M. Takahashi, and M. Kinoshita, *Chem. Phys. Lett.* **186**, 401 (1991).

<sup>10</sup>R. Chiarrelli, M. A. Novak, A. Rassat, and J. L. Tholence, *Nature (London)* **363**, 147 (1993).

<sup>11</sup>F. Palacio, G. Antorrena, M. Castro, R. Burriel, J. Rawson, J. N. B. Smith, N. Bricklebank, J. Novoa and C. Ritter, *Phys. Rev. Lett.* **79**, 2336 (1997).

<sup>12</sup>J. Luzon, J. Campo, F. Palacio, G. J. McIntyre, A. E. Goeta, E. Ressouche, C. M. Pask, and J. M. Rawson, *Physica B* **335**, 1 (2003).

<sup>13</sup>M. Kinoshita, *Philos. Trans. R. Soc. London A* **357**, 2855 (1999).

<sup>14</sup>BImNN is 2-(benzimidazol-2-yl)-4,4,5,5-tetramethyl-4,5-dihydro-1H-imidazole-3-oxide-1-oxyl. In Refs. 17 and 29 it was given the

abbreviation 2-BIMNN, but here we follow the conventions of Refs. 18–22.

<sup>15</sup>N. Yoshioka, M. Irisawa, Y. Mochizuki, T. Kato, H. Inoue, and S. Ohba, *Chem. Lett.* **26**, 251 (1997).

<sup>16</sup>N. Yoshioka, M. Irisawa, Y. Mochizuki, T. Aoki, and H. Inoue, *Mol. Cryst. Liq. Cryst. Sci. Technol. A* **306**, 403 (1997).

<sup>17</sup>T. Sugano, S. J. Blundell, W. Hayes, and P. Day, *Polyhedron* **22**, 2343 (2003).

<sup>18</sup>H. Murata, Y. Miyazaki, A. Inaba, A. Paduan-Filho, V. Bindilatti, N. F. Oliveira, Jr., Z. Delen and P. M. Lahti, *J. Am. Chem. Soc.* **130**, 186 (2008).

<sup>19</sup>H. Murata, Z. Delen, and P. M. Lahti, *Chem. Mater.* **18**, 2625 (2006).

<sup>20</sup>H. Murata, J. T. Mague, S. Aboaku, N. Yoshioka, and P. M. Lahti, *Chem. Mater.* **19**, 4111 (2007).

<sup>21</sup>G. Seber, R. S. Freitas, J. T. Mague, A. Paduan-Filho, X. Gratsens, V. Bindilatti, N. F. Oliveira, Jr., N. Yoshioka and P. M. Lahti, *J. Am. Chem. Soc.* **134**, 3825 (2012).

<sup>22</sup>G. Seber, G. J. Halder, J. A. Schlueter, and P. M. Lahti, *Cryst. Growth Des.* **11**, 4261 (2011).

<sup>23</sup>S. F. J. Cox, *J. Phys. C* **20**, 3187 (1987); S. J. Blundell, *Contemp. Phys.* **40**, 175 (1999); P. Dalmas de Réotier and A. Yaouanc, *J. Phys. C* **9**, 9113 (1997).

<sup>24</sup>T. Lancaster, S. J. Blundell, M. L. Brooks, P. J. Baker, F. L. Pratt, J. L. Manson, C. P. Landee, and C. Baines, *Phys. Rev. B* **73**, 020410(R) (2006).

<sup>25</sup>J. L. Manson, T. Lancaster, L. C. Chapon, S. J. Blundell, J. A. Schlueter, M. L. Brooks, F. L. Pratt, C. L. Nygren, and J. S. Qualls, *Inorg. Chem.* **44**, 989 (2005).

<sup>26</sup>S. J. Blundell, P. A. Pattenden, R. M. Valladares, F. L. Pratt, T. Sugano, and W. Hayes, *Solid State Commun.* **92**, 569 (1994).

<sup>27</sup>A. J. Steele, T. Lancaster, S. J. Blundell, P. J. Baker, F. L. Pratt, C. Baines, M. M. Conner, H. I. Southerland, J. L. Manson, and J. A. Schlueter, *Phys. Rev. B* **84**, 064412 (2011).

- <sup>28</sup>S. J. Blundell, T. Lancaster, F. L. Pratt, P. J. Baker, M. L. Brooks, C. Baines, J. L. Manson, and C. P. Landee, *J. Phys. Chem. Solids* **68**, 2039 (2007).
- <sup>29</sup>T. Sugano, S. J. Blundell, T. Lancaster, F. L. Pratt, and H. Mori, *Phys. Rev. B* **82**, 180401(R) (2010).
- <sup>30</sup>S. J. Blundell, P. A. Pattenden, F. L. Pratt, R. M. Valladares, T. Sugano, and W. Hayes, *Europhys. Lett.* **31**, 573 (1995).
- <sup>31</sup>J. H. Brewer, S. R. Kreitzman, D. R. Noakes, E. J. Ansaldo, D. R. Harshman, and R. Keitel, *Phys. Rev. B* **33**, 7813 (1986).
- <sup>32</sup>T. Lancaster, F. L. Pratt, S. J. Blundell, I. McKenzie, and H. E. Assender, *J. Phys.: Condens. Matter* **21**, 346004 (2009).
- <sup>33</sup>J. S. Möller, D. Ceresoli, T. Lancaster, N. Marzari, and S. J. Blundell, *Phys. Rev. B* **87**, 121108(R) (2013).
- <sup>34</sup>F. Bernardini, P. Bonfá, S. Massidda, and R. De Renzi, *Phys. Rev. B* **87**, 115148 (2013).
- <sup>35</sup>P. Giannozzi, S. Baroni, N. Bonini, M. Calandra, R. Car, C. Cavazzoni, D. Ceresoli, G. L. Chiarotti, M. Cococcioni, I. Dabo, A. Dal Corso, S. de Gironcoli, S. Fabris, G. Fratesi, R. Gebauer, U. Gerstmann, C. Gougoussis, A. Kokalj, M. Lazzeri, L. Martin-Samos, N. Marzari, F. Mauri, R. Mazzarello, S. Paolini, A. Pasquarello, L. Paulatto, C. Sbraccia, S. Scandolo, G. Sclauzero, A. P. Seitsonen, A. Smogunov, P. Umari, and R. M. Wentzcovitch, *J. Phys.: Condens. Matter* **21**, 395502 (2009).
- <sup>36</sup>J. P. Perdew, K. Burke, and M. Ernzerhof, *Phys. Rev. Lett.* **77**, 3865 (1996).
- <sup>37</sup>D. Vanderbilt, *Phys. Rev. B* **41**, 7892 (1990).
- <sup>38</sup>Y. Nakazawa, M. Tamura, N. Shirakawa, D. Shiomi, M. Takahashi, M. Kinoshita, and M. Ishikawa, *Phys. Rev. B* **46**, 8906 (1992).
- <sup>39</sup>H. A. Algra, L. J. de Jongh, W. J. Huiskamp, and R. L. Carlin, *Physica B + C* **92**, 187 (1977).
- <sup>40</sup>D. D. Swank, C. P. Landee, and R. D. Willett, *Phys. Rev. B* **20**, 2154 (1979).
- <sup>41</sup>R. D. Willett and C. P. Landee, *J. Appl. Phys.* **52**, 2004 (1981).
- <sup>42</sup>K. Takeda, K. Konishi, K. Nedachi, and K. Mukai, *Phys. Rev. Lett.* **74**, 1673 (1995).
- <sup>43</sup>R. D. Willett, C. P. Landee, R. M. Gaura, D. D. Swank, H. A. Groenendijk, and A. J. van Duynveldt, *J. Magn. Magn. Mater.* **15–18**, 1055 (1980).
- <sup>44</sup>J. C. Schouten, G. J. van der Geest, W. J. M. de Jonge, and K. Kopinga, *Phys. Lett. A* **78**, 398 (1980).
- <sup>45</sup>K. Takeda, T. Hamano, T. Kawae, M. Hidaka, M. Takahashi, S. Kawasaki, and K. Mukai, *J. Phys. Soc. Jpn.* **64**, 2343 (1995).
- <sup>46</sup>C. P. Landee and R. D. Willett, *Phys. Rev. Lett.* **43**, 463 (1979).
- <sup>47</sup>C. Dupas, J. P. Renard, J. Seiden, and A. Cheikh-Rouhou, *Phys. Rev. B* **25**, 3261 (1982).
- <sup>48</sup>K. Kopinga, A. M. C. Tinus, and W. J. M. de Jonge, *Phys. Rev. B* **25**, 4685 (1982).